Effect of Thermal and Mechanical Processing on Molecular Ordering in Liquid Crystal Elastomers

Liquid crystalline polymers have been the focus of intensive research in recent years because of their potential for use in a wide range of optical as well as photonic applications.[1–3] Although the macroscopic alignment required for practical applications can be achieved by surface treatment and the application of an external electric or magnetic field, the effectiveness of these processing techniques is limited to films with a thickness less than 100 μm.[4] To overcome this problem, liquid crystalline (LC) *elastomers* have been explored in view of the relative ease with which mesogenic moieties can be aligned by stretching.[5–11] An additional feature of these materials is the ability to "lock-in" this stress-induced alignment via crosslinking of reactive side-chains to produce a three-dimensional polymer network.

Finkelmann *et al.*[12] have previously described a novel two-stage reaction scheme for the preparation of LC elastomers; this process is shown in Fig. 61.35. In the first stage, a hydrosilylation reaction was conducted on the terminal methylene groups of the polymer to obtain a partially crosslinked elastomer carrying two pendant groups: a nematogen and a methacrylate. In the second stage, a constant stress was applied to produce uniform nematic alignment followed by a second crosslinking step by means of the less-reactive methacryloyl groups. Poly(methylhydrosiloxane), with a degree of polymerization n of 120, was employed exclusively in these experiments.

In this article we describe the preparation of mesogenic elastomer systems based on two commercially available polysiloxanes, poly(methylhydrosiloxane) (n = 40) and poly(ethylhydrosiloxane) (n = 80), and their characterization by Fourier transform infrared (FTIR) spectroscopy, differential scanning calorimetry (DSC), hot-stage polarized optical microscopy, stress-strain analysis, and x-ray diffraction to elucidate the dynamic features of preparation and processing of LC elastomers.

Experimental Section

1. Materials

Poly(methylhydrosiloxane) (PMHS), $-[(CH_3)SiH-O-]_{40}-$, (0.30 Stoke, Spectrum Chemicals); poly(ethylhydrosiloxane) (PEHS), $-[(C_2H_5)SiH-O-]_{80}-$, (1.00 Stoke, Gelest); toluene (anhydrous, 99+% Aldrich Chemical Company); and a Pt-catalyst (PC072, United Chemical Technologies) were all used as received without further purification. The nematic monomer and cross-linking agents were synthesized by standard literature methods, as shown in Figs. 61.36 and 61.37.

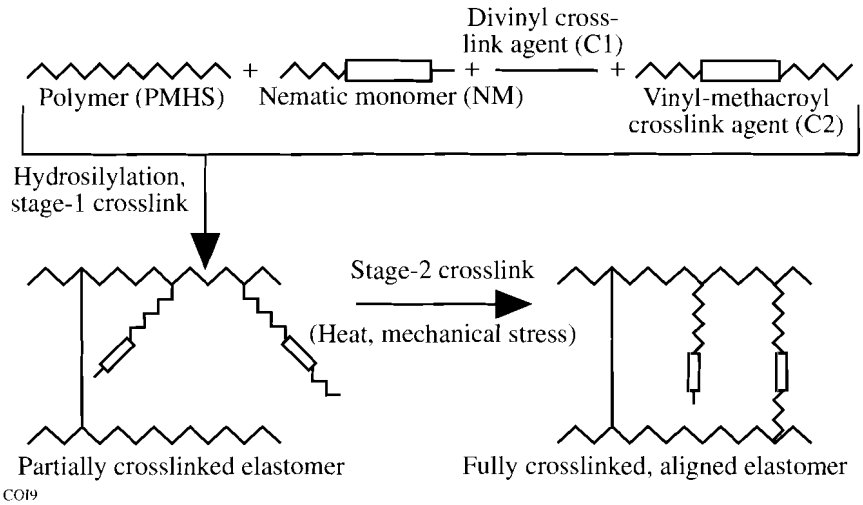

Figure 61.35
The two-step process for the preparation of aligned LC elastomers. The components are combined and reacted to form a partially crosslinked elastomer; the combination of heat and mechanical stress completes the crosslinking reaction and aligns the mesogenic pendant groups.

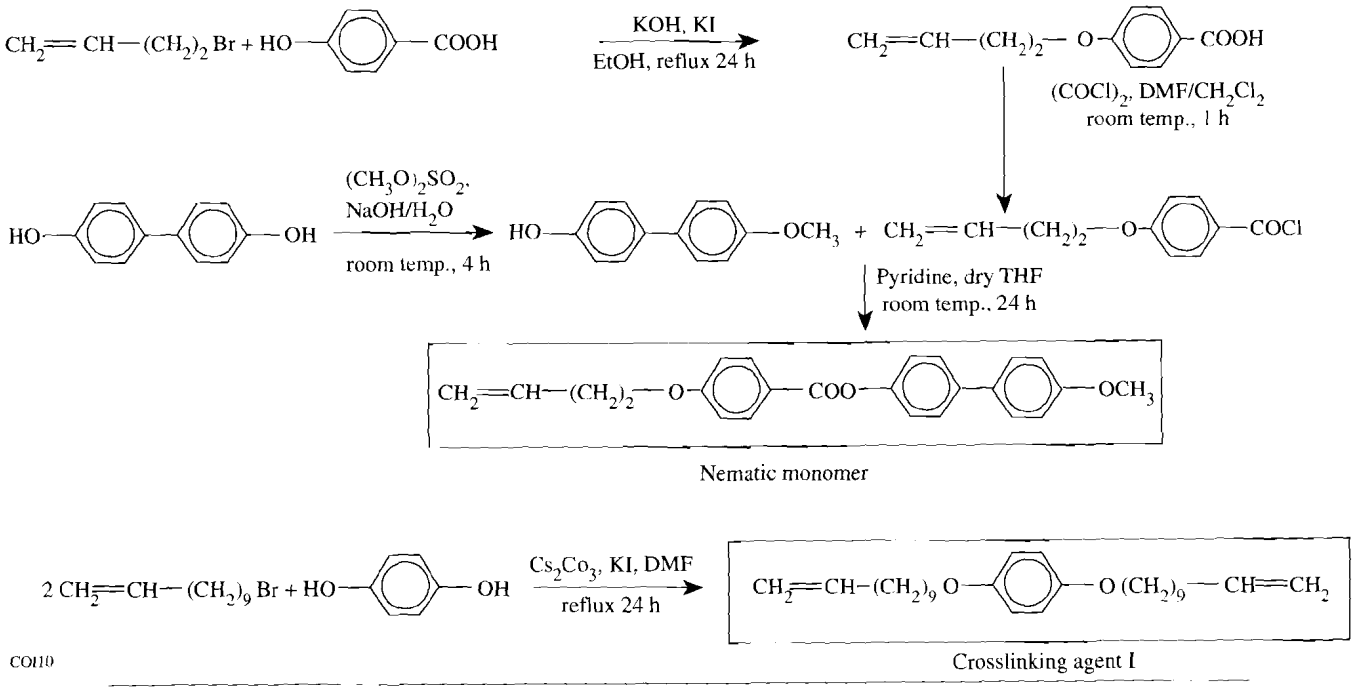

Figure 61.36
Synthesis scheme for the preparation of the nematic monomer and the diacrylate crosslinking agent used for elastomer preparation.

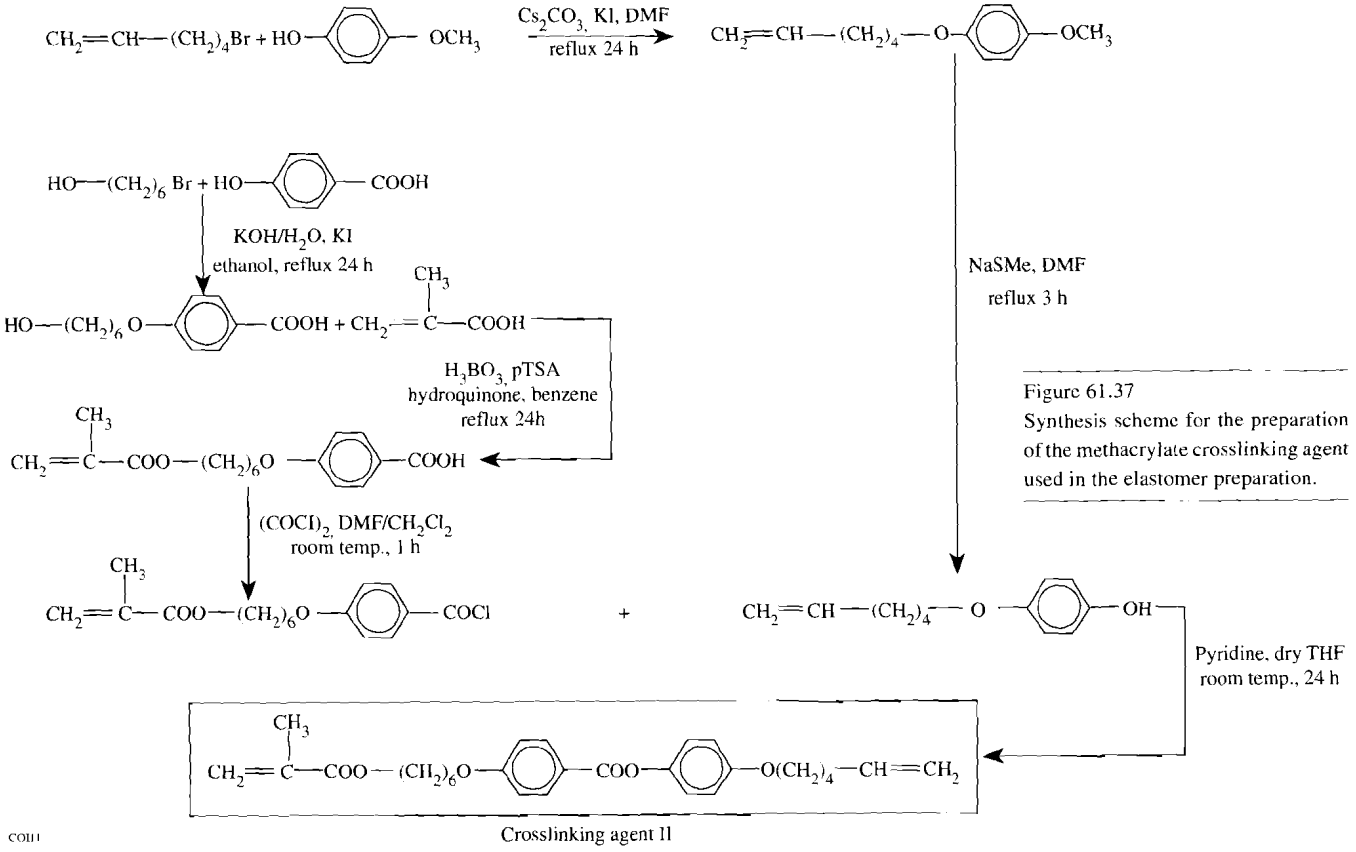

Figure 61.37
Synthesis scheme for the preparation of the methacrylate crosslinking agent used in the elastomer preparation.

2. Preparation of Elastomers

To prepare the elastomers, appropriate quantities of the nematic monomer (NM), the first crosslinking agent (C1), and the second crosslinking agent (C2), as shown in Fig. 61.38, were added to PEHS or PMHS in a round-bottomed reaction flask to ensure a polymer:NM:C1:C2 molar ratio of 1:0.3:0.1:0.1. Upon addition of toluene (13.6 ml/g-material), the flask was sealed, flushed with nitrogen, and heated to ensure dissolution of solids. The catalyst was added ([Pt/CH_2 = CH–] ≈ 0.002), and the flask was shaken vigorously for 30 s before quickly transferring the contents to a heated Teflon™ mold kept overnight at 60°C under a nitrogen purge (first-stage reaction). The elastomer was carefully removed from the mold, stretched by the desired amount, and left for three days on a hot plate at 60°C to complete the elastomer preparation (second-stage reaction). This method of elastomer preparation is similar to that reported by Finkelmann *et al.*,[12] with the exception that a constant *strain*, as opposed to a constant *stress*, was used in our experiments. The extent of reaction was monitored using FTIR spectroscopy. The elastomers prepared from PEHS and PMHS parent polymers were denoted as ES and MS, respectively.

3. Methods of Characterization

The degrees of polymerization of PEHS and PMHS were evaluated from a viscosity versus molecular weight relationship derived from product data (United Chemical Technologies). Infrared spectra of both the parent polymers and the elastomers were obtained using a Nicolet 20SXC FTIR spectrophotometer. Differential scanning calorimetry (DSC) data were collected using a Perkin Elmer DSC-4 at +20°C/min under a helium purge with liquid nitrogen cooling. A hot-stage polarized optical microscope (Leitz Orthoplan-Pol and a Mettler FP52 hot stage) was used for mesophase identification and verification of transition temperatures determined by DSC. Mechanical characterization of elastomers was conducted in a water bath at 55±1°C using an Instron Table Model 1102 instrument. The stress σ is determined in terms of the original cross sectional area, and the strain is defined as $\varepsilon = (l - l_0)/l_0$, where l and l_0 are the length at the time of data collection and original length, respectively.

Two-dimensional, flat-plate x-ray diffraction patterns were collected using a Statton box camera with a sample-to-film distance of 5.0 cm. An image-plate storage phosphor detector was utilized in place of x-ray film to reduce data-collection time.[13] Samples were irradiated with nickel-filtered copper radiation. A qualitative assessment of orientation and liquid crystallinity was accomplished using the flat-plate diffraction data. The x-ray diffraction patterns were obtained with a Rigaku RU-300 pole figure goniometer used in the Bragg-Brentano geometry. This diffractometer was equipped with a copper rotating anode operated at 50 kV and 280 mA, a diffracted-beam nickel filter, and a scintillation detector. Reflection-mode $\theta/2\theta$ scans provided information on planar orientation, while symmetrical transmission-mode $\theta/2\theta$ scans provided a preliminary assessment of in-plane orientation. A quantitative orientation analysis was performed by an azimuthal diffraction technique.[14] Data were collected using the Rigaku RU-300 pole goniometer as mentioned above. Azimuthal analysis involved positioning a sample at a fixed angle θ in the symmetric transmission mode with the detector

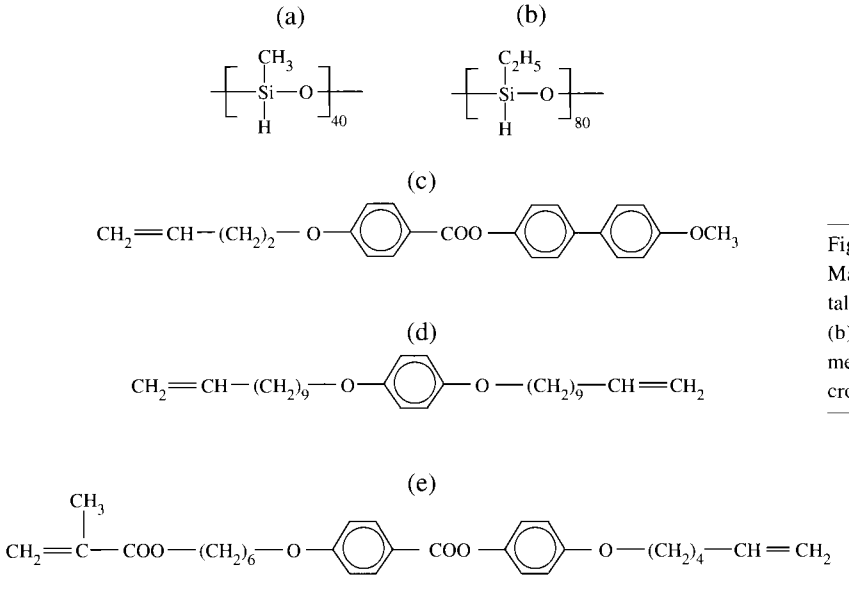

Figure 61.38
Materials used in the preparation of the liquid crystalline elastomers: (a) poly(methylhydrosiloxane); (b) poly(ethylhydro-siloxane); (c) nematic monomer; (d) first crosslinking agent; and (e) second crosslinking agent.

COH2

at a fixed 2θ to detect a desired Bragg diffraction peak. The sample was then rotated 360° around the normal to the sample plane, defined as the χ rotation. In this study the transverse direction was mounted at zero azimuthal angle, i.e., parallel to the plane of the x-ray beam. Azimuthal data allowed the determination of in-plane orientation. Orientation distribution was quantified by the use of the Herman's orientation distribution function (HOF_A) defined for in-plane alignment as[14]

$$HOF_A = \frac{3\langle\cos^2\chi\rangle - 1}{2} \quad (1)$$

with $\langle\cos^2\chi\rangle$ defined as

$$\langle\cos^2\chi\rangle = \frac{\Sigma I(\chi)\sin\chi\cos^2\chi}{\Sigma I(\chi)\sin\chi}, \quad (2)$$

where $I(\chi)$ denotes intensity as a function of azimuthal angle χ. The value of HOF_A ranges from –0.5 to 1 for in-plane orientation distribution, with a value of –0.5 indicating a perfect alignment of polymer chains along the strain direction, a value of 0 indicating a random or balanced alignment, and a value of 1 indicating perfect alignment of polymer chains along the transverse direction.[14]

Results and Discussion

Fourier transform infrared spectrometry was used to monitor the extent of hydrosilylation reaction, as illustrated in Fig. 61.39 for elastomer MS, where a comparison of scans recorded after the first- [Fig. 61.39(a)] and second-stage [Fig. 61.39(b)] reactions shows the expected reduction in the intensity of the Si-H stretching band at 2160 cm^{-1}. The effect of reaction on the mechanical properties of both the ES and MS elastomers is illustrated in the stress versus strain curves of Fig. 61.40. In light of the reported effect of crosslink density on glass transition (T_g) and liquid-crystal-to-isotropic transition temperatures,[4–11] it is important to ensure that a valid comparison of ES to MS elastomers is made. The crosslink density in terms of the molecular weight between crosslinks, M_c, is related to the elastic modulus E (N/mm^2) at low strains and at temperatures above T_g by Eq. (3):[6]

$$E = \frac{3\rho RT}{M_c}, \quad (3)$$

where ρ is the density estimated at 1.0 g/cm^3,[8,11] R the ideal gas constant, and T the temperature (°K). Since the data were collected at a temperature (55°C) that is above the T_g for all samples considered, Eq. (3) is appropriate for evaluating E from Fig. 61.40. Using Eq. (3), an M_c of 660 g/mole (E = 12.4 N/mm^2) and 560 g/mole (E = 14.6 N/mm^2) were found for the ES and MS elastomers, respectively. Figure 61.37 also shows the expected increase in E (*i.e.*, a decrease in M_c) with an increased extent of reaction. Since samples must be stretched during the second-stage reaction to achieve bulk alignment of the nematic pendant groups, the maximum strain sustained, ε_b, is an important parameter. For our elastomer composition as defined earlier, ES and MS possessed an ε_b value of 0.31 and 0.16, respectively. The difference in ε_b is attributed to the higher molecular weight of the ES system since the degrees of polymerization of the PEHS and PMHS polymers are 80 and 40, respectively.

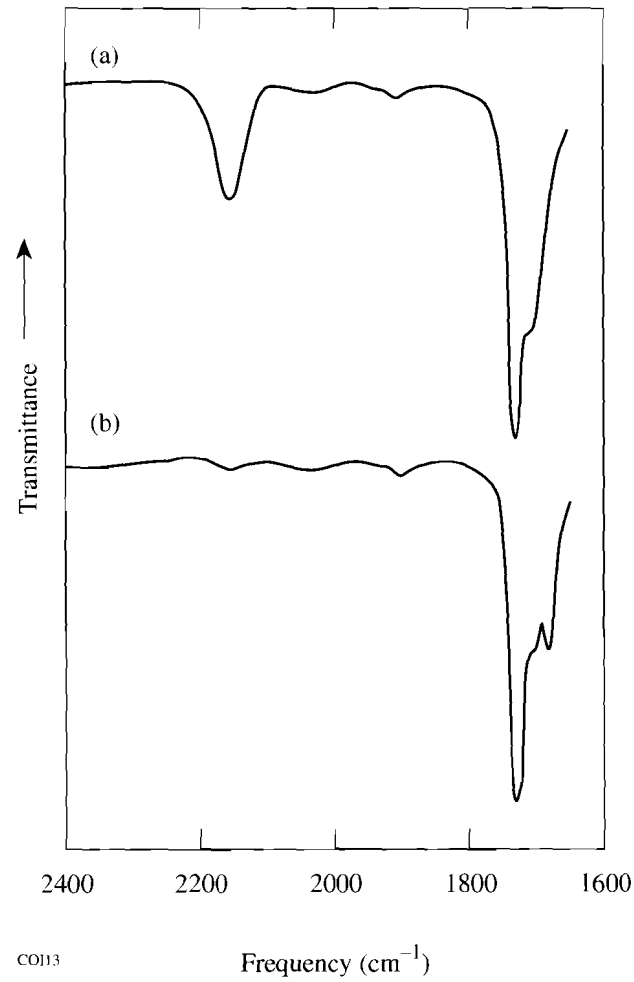

Figure 61.39
FTIR spectra of the MS elastomer after (a) first-stage and (b) second-stage reaction.

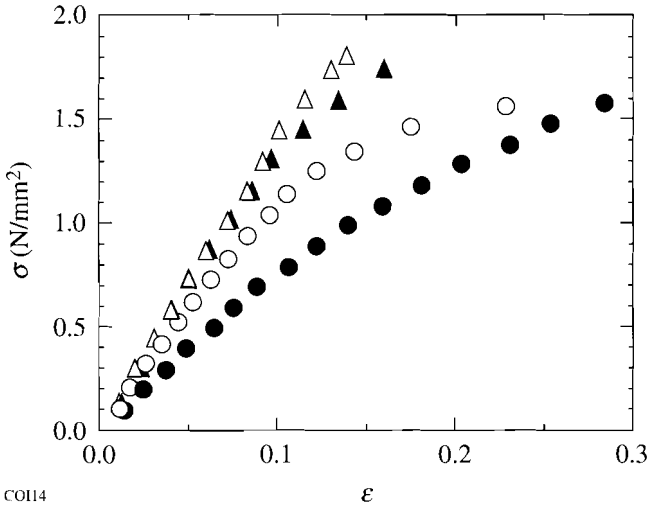

Figure 61.40
Stress (σ) versus strain (ε) recorded at 55°C for MS elastomer after first-stage (▲) and second-stage reaction (△), and ES elastomer after first-stage (●) and second-stage reaction (○).

The DSC thermograms of ES and MS are presented in Fig. 61.41, where the subscripts *s* and *n* refer to samples that were stretched and not stretched, respectively, during the second-stage reaction. Samples described as "stretched" are those that were strained to the fullest possible extent without tearing during the second-stage reaction. Since the glass transitions of pure PEHS and PMHS are −149°C and −140°C, respectively, the substitution and crosslinking reactions would appear to be responsible for the elevated glass transitions of both polymer hosts. This factor is consistent with the increase in *E* observed in Fig. 61.40. In the first heating scan of the ES elastomer prepared without stretching, an endotherm occurs at 82°C [Fig. 61.41(a)] due to a nematic-to-isotropic transition. A lower value for the transition enthalpy (ΔH) was obtained for an equivalent sample that had been stretched. After the ES sample is heated through this transition temperature and slowly cooled to room temperature, the nematic-isotropic endotherm now appears at 63°C [Fig. 61.38(b)] with a greatly reduced ΔH. If this same ES elastomer sample is instead rapidly cooled to low temperatures (i.e., quenched) from 90°C and then annealed at 60°C, subsequent heating gives an endotherm at 70°C with a ΔH of 1.9 J/g, identical to the value shown in Fig. 61.38(b). These results infer that the ΔH for the nematic-isotropic transition is independent of thermal history applied after the initial heating cycle, while, in contrast, the nematic-isotropic transition temperature ($T_{n\text{-}i}$) displays total thermal history dependence. For the MS elastomer [Fig. 61.41(c)], the endotherm at 80°C is accompanied by a reduced ΔH as compared to the ES elastomer, even though the nematic texture was clearly visible between T_g and 80°C by hot-stage polarizing microscopy. The absence of an endotherm for elastomer MS when the same sample is rescanned [Fig. 61.41(d)] suggests a lack of nematic ordering. Finkelmann *et al.*,[12] however, have reported values for T_g, $T_{n\text{-}i}$, and $\Delta H_{n\text{-}i}$ of 0°C, 83°C, and 1.7 J/g°K, respectively, for the elastomer prepared from PMHS with a degree of polymerization of 120. Other than the differences in the chain length of the starting PMHS and in the

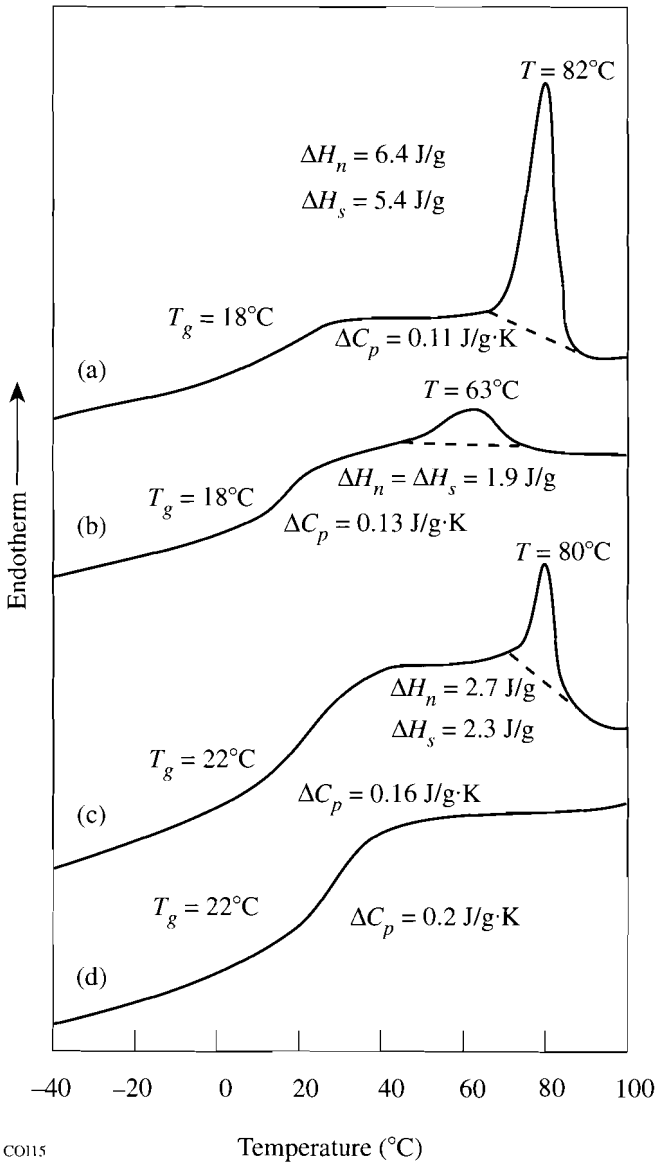

Figure 61.41
DSC thermograms recorded at 20°C/min. of (a) ES elastomer; (b) second heating scan of ES elastomer after the sample was first heated to 90°C and cooled at 5°C/min to room temperature; (c) MS elastomer; and (d) second heating scan of MS elastomer after the sample was heated to 90°C and cooled at 5°C/min to room temperature.

crosslink density, no explanation can be offered for the discrepancy with our experimental results. It appears that the observed values of ΔH_n and ΔH_s of the ES and MS elastomers without any previous thermal history are both greater than those that can be properly accounted for by a typical nematic-to-isotropic transition.

To gain further insights into the relationship between molecular ordering and the endotherms acquired during the first heating scans of the ES and MS elastomers, we turned to x-ray diffraction techniques. The flat-plate diffraction pattern for the unstretched ES sample [Fig. 61.42(a)] shows two broad diffraction rings characteristic of a polydomain nematic, as was also observed for the unstretched MS elastomer. Interplanar spacing calculations reveal that the inner and outer rings have d-spacings of 8.8 Å and 4.38 Å, respectively. Upon stretching the elastomers, in-plane orientation occurs, as evidenced by the formation of arcs in the flat-plate diffraction pattern for the ES elastomer with $\varepsilon = 0.3$ [Fig. 61.42(b)], which is characteristic of a monodomain nematic.[15] Due to the lower sustainable strains in the MS elastomer (see Fig. 61.40), the effect of strain on orientation in this system is not pronounced, as evidenced by the lack of arc formation in the flat-plate camera photographs. In the ES samples, the majority of the diffraction scatter lies in the equatorial position (zeroth order) in the flat-plate pattern, which indicates that the 8.8-Å and 4.38-Å diffraction peaks are of the type ($hk0$). In the following discussion, the term "thermal treatment" indicates that the samples were heated at 90°C for 10 min and then cooled to room temperature. Upon thermal treatment of the stretched ES elastomer, the nematic order is retained, as evidenced by the absence of any discernible effect on arc formation in comparing Figs. 61.42(b) and 61.42(c). In fact, the $\Delta H_{n\text{-}i}$ at 63°C, 1.9 J/g as noted in Fig. 61.41(b), is typical of a nematic-to-isotropic transition. Thus, the $\Delta H_{n\text{-}i}$ observed in Fig. 61.41(a) appears to be caused by a combination of nematic-to-isotropic transition and molecular relaxation.

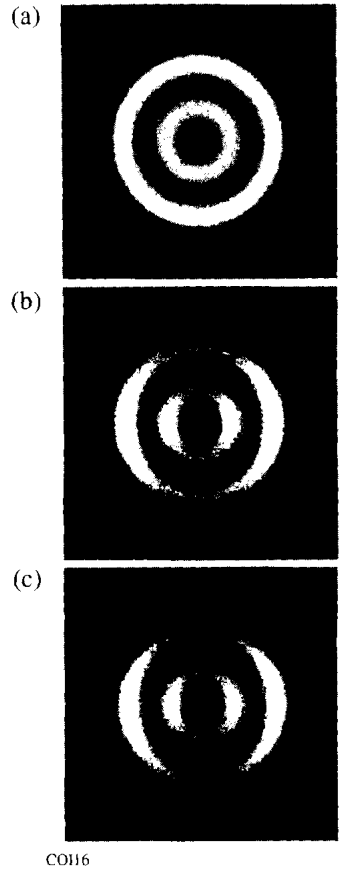

Figure 61.42
Flat-plate x-ray diffraction patterns of ES elastomer: (a) unstretched; (b) stretched to $\varepsilon = 0.3$; and (c) as in (b) but first heated to 90°C and then cooled to room temperature.

Transmission-mode x-ray diffraction data were collected for elastomer ES over a selected range of 2θ, as shown in Fig. 61.43. An inspection of Fig. 61.43 reveals that, for both unstretched [I(a)] and stretched [II(a)] ES samples, the 4.38-Å peak (corresponding to the outer ring shown in Fig. 61.42) observed in the flat-plate diffraction data actually comprises *two* peaks with d-spacings of 4.47 Å and 4.13 Å. The two peaks can be resolved because of the 20-cm sample-to-detector distance, as compared to the 5-cm distance utilized in the flat-plate diffraction work. The intensity of the 4.13-Å peak relative to that of the 4.47-Å peak is clearly diminished by stretching. The 4.13-Å peak disappears with an increase in intensity of the 4.47-Å peak with thermal treatment, as revealed in comparing I(b) to I(a) and II(b) to II(a) (Fig. 61.43). These observations indicate that stretching and thermal treatment may induce some degree of molecular relaxation, consistent with the facts that $\Delta H_n > \Delta H_s$ and that ΔH_n and ΔH_s both decrease to 1.9 J/g upon thermal treatment (see Fig. 61.41).

Azimuthal diffraction data collected on the 4.47-Å peak, as shown in Fig. 61.44, permit a quantitative assessment of molecular relaxation resulting in an enhanced order reflected by the HOF_A parameter defined by Eq. (1). These data suggest that the unstretched ES sample has no in-plane alignment, which implies a near-random distribution of lattice planes based on a HOF_A value of 0.02. For the stretched ES sample, the peaks at 0° and 180° azimuthal positions in Fig. 61.44 (along the sample transverse direction) and a HOF_A value of 0.35 reveal the effect of stretching on the preferred orientation of ($hk0$) lattice planes. Thermal treatment of the stretched sample shows an enhancement of the azimuthal intensity along the transverse direction, resulting in an increased HOF_A value of 0.43 apparently due to the alignment of nematic domains. To be consistent with the observed order in which the HOF_A value

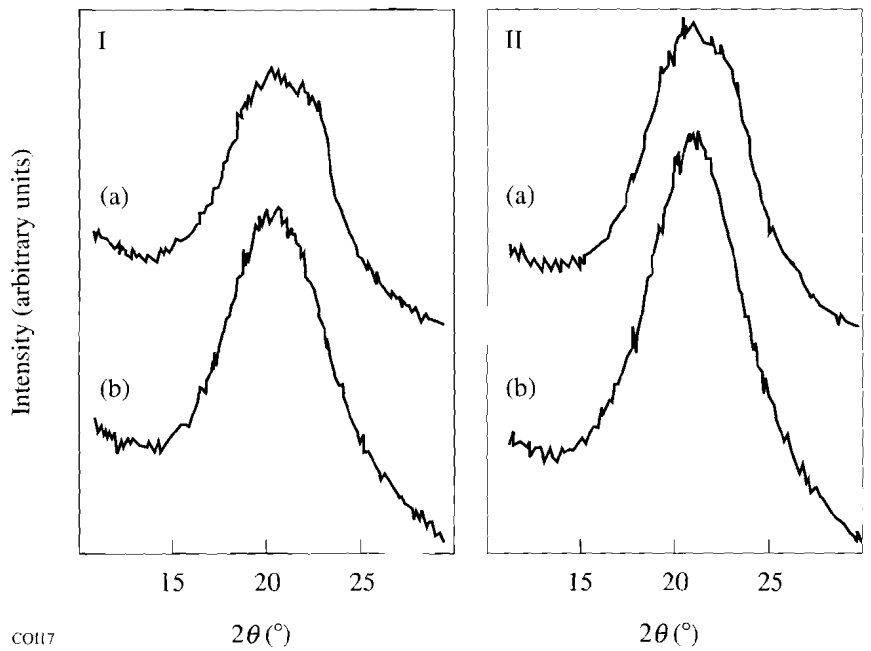

Figure 61.43
X-ray diffraction patterns of ES elastomer: I(a) unstretched, no thermal processing; I(b) sample I(a) heated at 90°C for 10 min and by cooled to room temperature; II(a) stretched to $\varepsilon = 0.3$, no thermal processing; II(b) stretched as in II(a) followed by heating at 90°C for 10 min and cooled to room temperature.

increases upon stretching and thermal treatment, the DSC thermograms in Figs. 61.41(a) and 61.41(b) should be interpreted in terms of stored enthalpy at the molecular scale that is released to some extent by stretching during the second-stage reaction and completely released by thermal treatment. This mode of enthalpy storage does not seem to contribute to the experimentally quantified HOF_A parameter on a relatively macroscopic scale in the case of nematic ordering.

From the x-ray diffraction and thermal analysis data reviewed above, we can make several observations regarding the effect of processing on mesomorphic behavior:

- Based on the flat-plate x-ray diffraction pattern, an imposed strain gives rise to a monodomain nematic character, whereas a polydomain character is observed in the absence of applied strain. Furthermore, the monodomain character achieved with the application of strain is retained when the sample is heated above the nematic-isotropic transition temperature and cooled back to room temperature.

- The DSC thermograms, coupled with the transmission-mode x-ray diffraction data, suggest that (a) enthalpy is stored in the freshly prepared elastomer; (b) the imposed strain helps to release the stored enthalpy to some extent; and (c) the stored enthalpy is almost completely released upon thermal cycling between the nematic-isotropic transition and room temperature.

- The transmission mode and azimuthal x-ray diffraction data demonstrate that, although the stored enthalpy does not lead to an increased order parameter (HOF_A), the enthalpy is released through molecular relaxation upon stretching or thermal treatment. This enthalpy release appears to enhance nematic ordering and increase HOF_A values.

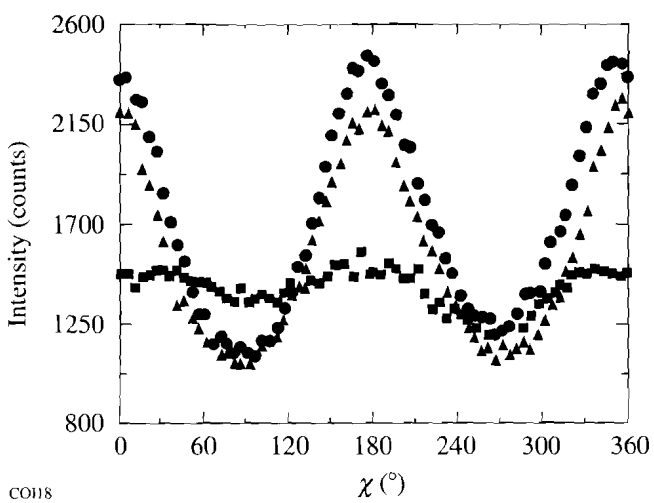

Figure 61.44
X-ray diffraction azimuth plots for ES elastomer at $2\theta = 19.8°$, i.e., the 4.47-Å peak in Fig. 61.40: unstretched (■), stretched to $\varepsilon = 0.3$ (▲), and stretched to $\varepsilon = 0.3$ (●) while heating at 90°C for 10 min followed by cooling to room temperature.

Summary

Liquid crystalline elastomers derived from siloxane polymers, PMHS and PEHS, were prepared following a two-stage reaction scheme to investigate the effects of processing conditions and thermal treatment on mesomorphic characteristics. A thorough analysis of these elastomers by a combination of FTIR, DSC, mechanical analysis, polarized hot-stage optical microscopy, and x-ray diffraction techniques has shown that the chain length of the precursor siloxane polymer plays an important role in achieving bulk alignment via stretching during the second-stage reaction. The imposed strain was also demonstrated to be critical in achieving a monodomain nematic character, which is completely recoverable after repeated thermal cycling from $T_{n\text{-}i}$ to room temperature. The latter feature is especially important in the preparation of freestanding, optical-quality birefringent films for laser and other optical device applications.

ACKNOWLEDGMENT

This work was supported in part by the Army Research Office under Contract #DAAL03-92-G-0147, the Contact Lens Division of Bausch & Lomb, Inc., the U.S. Department of Energy Office of Inertial Confinement Fusion under Cooperative Agreement No. DE-FC03-92SF19460, and the University of Rochester. The support of DOE does not constitute an endorsement by DOE of the views expressed in this article. The authors would like to thank Craig Barnes of Eastman Kodak Company for assistance in gathering the x-ray data, Eric J. Leibenguth and Linda Slapelis of Bausch & Lomb for assistance in the stress-strain analysis, Dr. Jay F. Kunzler of Bausch & Lomb for helpful discussions, Darin Phelps of the Department of Chemical Engineering for assistance in monomer synthesis, and Professor Burns of the Department of Mechanical Engineering, University of Rochester for helpful discussions.

REFERENCES

1. (a) H. Finkelmann, Angew. Chem. Int. Ed. Engl. **26**, 816 (1987); (b) H. Finkelmann, in *Liquid Crystallinity in Polymers: Principles and Fundamental Properties*, edited by A. Ciferri (VCH Publishers, New York, 1991), p. 315.
2. G. W. Gray, in *Side Chain Liquid Crystal Polymers*, edited by B. McArdle (Chapman and Hall, New York, 1989), p. 106.
3. V. Percec and Q. Zheng, J. Mater. Chem. **2**, 475 (1992).
4. J. Schätzle and H. Finkelmann, Mol. Cryst. Liq. Cryst. **142**, 85 (1987).
5. W. Gleim and H. Finkelmann, in *Side Chain Liquid Crystal Polymers*, edited by C. B. McArdle (Chapman and Hall, New York, 1989), p. 287.
6. F. J. Davis, J. Mater. Chem. **3**, 551 (1993).
7. M. Brehmer and R. Zentel, Mol. Cryst. Liq. Cryst. **243**, 353 (1994).
8. T. Tsutsui and R. Tanaka, Polymer **22**, 117 (1981).
9. (a) R. Zentel and M. Benalia, Makromol. Chem. **188**, 665 (1987); (b) R. Zentel and G. Reckert, Makromol. Chem. **187**, 1915 (1986).
10. H. Loth and A. Euschen, Makromol. Chem., Rapid Commun. **9**, 35 (1988).
11. (a) J. Küpfer and H. Finkelmann, Macromol. Chem. Phys. **195**, 1353 (1994); (b) J. Schätzle, W. Kaufhold, and H. Finkelmann, Makromol. Chem. **190**, 3269 (1989); (c) H. Finkelmann, H.-J. Kock, and G. Rehage, Makromol. Chem., Rapid Commun. **2**, 317 (1981).
12. J. Küpfer and H. Finkelmann, Makromol. Chem., Rapid Commun. **12**, 717 (1991).
13. T. N. Blanton, in *Advances in X-Ray Analysis* (Plenum Press, New York, in press), Vol. 37.
14. L. E. Alexander, *X-Ray Diffraction Methods in Polymer Science* (Wiley-Interscience, New York, 1969).
15. J. Falgueirettes and P. DeLord, in *Liquid Crystals & Plastic Crystals, Vol 2: Physicochemical Properties and Methods of Investigation*, edited by G. W. Gray and P. A. Winsor (Halsted Press, New York, 1974), p. 63.